

Supplementary information

Fast singlet excited-state deactivation pathway of flavin with a trimethoxyphenyl derivative

Stanisław Niziński ^{a,b}, Naisargi Varma ^c, Marek Sikorski ^{c,*},

Tomáš Tobrman ^d, Eva Svobodová ^d, Radek Cibulka ^{d,*}, Michał F. Rode ^{e,*}, Gotard Burdzinski ^{b,*}

^a Department of Biomolecular Mechanisms, Max Planck Institute for Medical Research,
Jahnstrasse 29, 69120 Heidelberg, Germany

^b Faculty of Physics and Astronomy, Adam Mickiewicz University, Uniwersytetu Poznanskiego 2,
61-614 Poznan, Poland

^c Faculty of Chemistry, Adam Mickiewicz University, Uniwersytetu Poznanskiego 8, 61-614
Poznan, Poland

^d Department of Organic Chemistry, University of Chemistry and Technology, Prague, 16628
Prague, Czech Republic

^e Institute of Physics, Polish Academy of Sciences, Aleja Lotników 32/46, 02-668 Warsaw, Poland

* Corresponding authors

E-mail addresses: sikorski@amu.edu.pl (M. Sikorski), radek.cibulka@vscht.cz (R. Cibulka),

mrode@ifpan.edu.pl (M. F. Rode), gotardeb@amu.edu.pl (G. Burdzinski)

Details of fluorescence up-conversion spectrometer

Fluorescence decay kinetics were collected using a custom-built time-resolved fluorescence up-conversion spectroscopy setup. Fundamental beam (100 fs pulses, 1 kHz repetition, 5.3 mm FWHM diameter, power of ≈ 3 W) is generated using Spitfire Ace Ti:sapphire regenerative amplifier (Spectra Physics), seeded by Tsunami Ti:sapphire oscillator (Spectra Physics) and pumped by Q-switched DPSS Ascend laser (Spectra Physics). Tsunami oscillator is pumped by 5W Millennia eV DPSS laser (Spectra Physics). Fundamental beam is split in the 90/10 ratio (Figure S1). Gate pulses are prepared using 90% of the fundamental beam. They travel through the delay line 4 times (forward and backward two times). After the delay line, diameter of the gate beam is decreased to about 2mm (FWHM) by the aperture, and beam polarization is adjusted using a half-wave plate. Finally, gate beam travels through up-conversion BBO crystal ($\theta = 34.7^\circ$, $\phi = 90^\circ$, 0.5 mm thickness, Eksma Optics), and is terminated on diaphragm. Pump pulses are prepared using 10% of the fundamental beam, which is attenuated and then frequency-doubled in BBO crystal ($\theta = 29.2^\circ$, $\phi = 90^\circ$, 0.5 mm thickness, Eksma Optics). Pump pulses of 400 nm generated this way are filtered to remove residual 800 nm pulses, using multiple reflections from dichroic mirrors. Furthermore, pump beam travels through the chopper and half-wave plate, which sets pump polarization to a magic angle with respect to the gate polarization. Finally, it is focused in the sample ($f=500$ mm) to a spot of about 400 μ m width (FWHM). Pulse energy is set to 250nJ. The sample is located in a 2mm cuvette (Hellma) and constantly stirred. Fluorescence light is collimated by 50mm lens and focused in up-conversion BBO crystal using 250mm lens. Fluorescence is additionally filtered by a 400nm notch filter, which removes residual pump beam. Collimated gate beam travels above fluorescence beam before entering upconverting BBO crystal. BBO crystal performs sum frequency generation using type I noncollinear phase matching, and it is mounted on rotational stage (Newport), which allows to select wavelength of fluorescence detection. The direction of generated up-converted UV beam is located between directions of the gate and fluorescence beams. After up-converting BBO crystal, sum frequency beam of the sample fluorescence and gate is spatially separated from other beams using the diaphragm, then collimated ($f=200$ mm) and focused ($f=150$ mm) in the monochromator (Andor Shamrock SR-163). Additional filtration is provided by one dichroic mirror (275-380nm) and two UG 11 filters (Thorlabs). The monochromator finally selects the up-converted light and directs it towards the photomultiplier (Hamamatsu R1527), powered by Stanford Research PS310 high voltage power supply. Signal produced by the photomultiplier is fed to the lock-in amplifier (Stanford Research SR830), which extracts signal components according to the frequency signal delivered by the pump chopper. The rotation angle of the up-converting BBO crystal and position of the delay stage are controlled by ESP300 controller (Newport). Both ESP300 motion controller and lock-in amplifier are computer-controlled using custom Python application, which controls experiment execution. Fluorescence kinetics are measured by bidirectional scanning of the gate-pump delays, and measuring light intensity component associated with pump modulation frequency registered by the photomultiplier. The instrument response function is about 400 fs. Fluorescence spectral resolution is mostly determined by geometry of the gate and fluorescence beams focused in the upconverting BBO crystal, and equals about 35nm (FWHM).

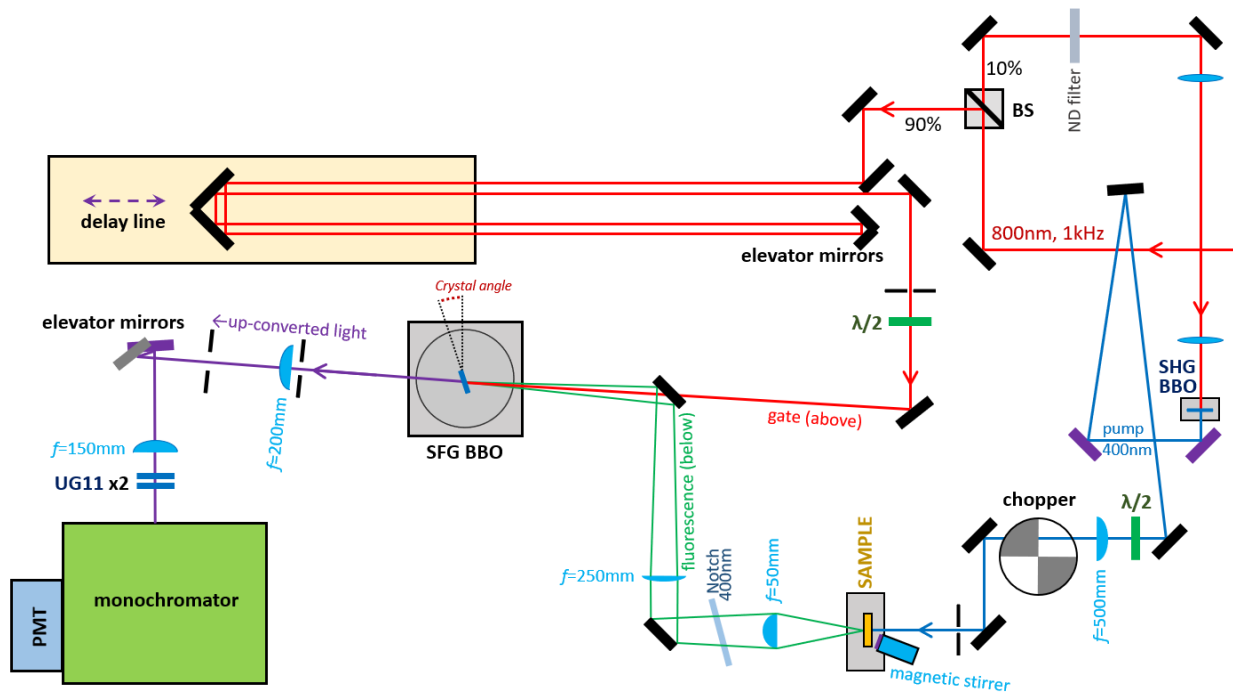
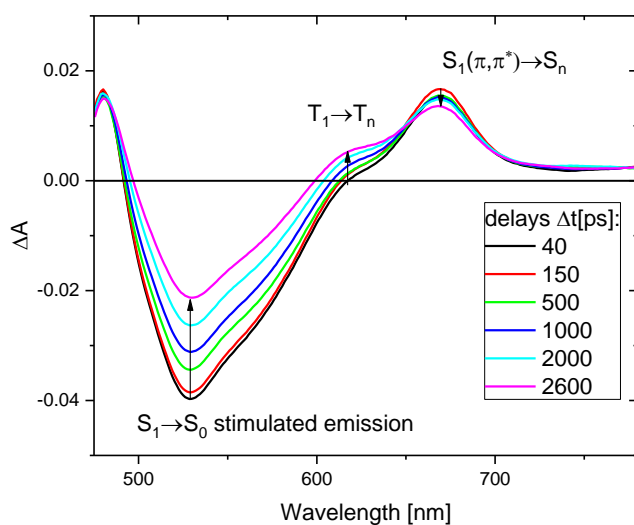
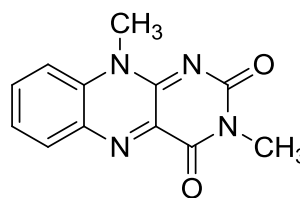


Figure S1. Fluorescence up-conversion spectrometer

A**B**

The photophysical processes:

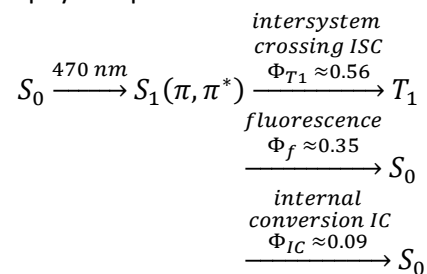
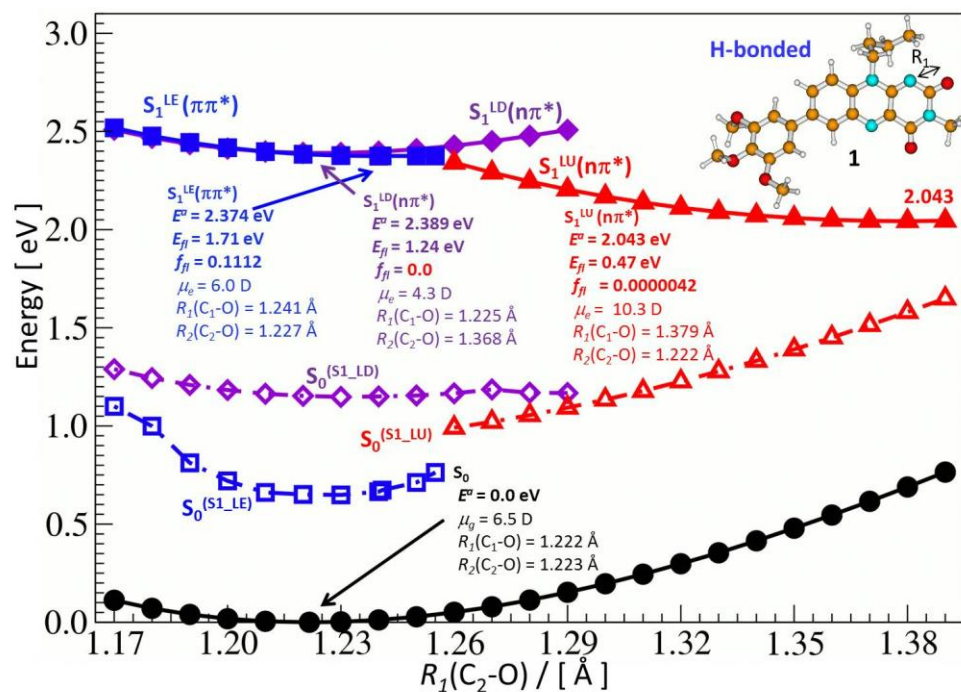
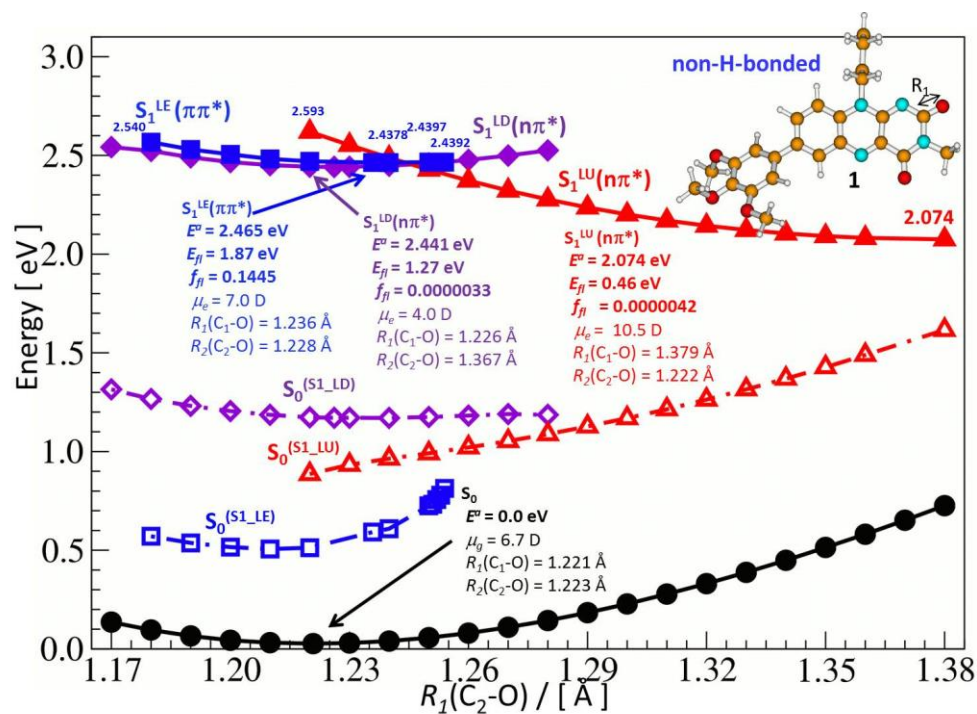


Figure S2. (A) Transient absorption data recorded in the visible range for **4** (3,10-dimethylisoalloxazine, $c=8 \times 10^{-4}$ M) in acetonitrile upon excitation at 470 nm (1 μ J). (B) The S_1 state is a long-lived population ($\tau_{S1} = 6.96$ ns accordingly to Ref. 15) and decays only partially in our 2.6 ns time window (limit of our instrument). Three deactivating channels for the S_1 state population are operational: (1) the $S_1 \rightarrow T_1$ intersystem-crossing, the quantum yield for triplet formation is estimated as a close value to the singlet oxygen quantum yield ($\Phi_{\Delta}=0.56$ in acetonitrile, ref. 15) (2) Fluorescence $S_1 \rightarrow S_0$ path (fluorescence quantum yield $\Phi_f=0.35$ in acetonitrile, Ref. 15) and (3) $S_1 \rightarrow S_0$ internal conversion process (yield Φ_{IC} estimated from relation $\Phi_{T1} + \Phi_f + \Phi_{IC} = 1$).

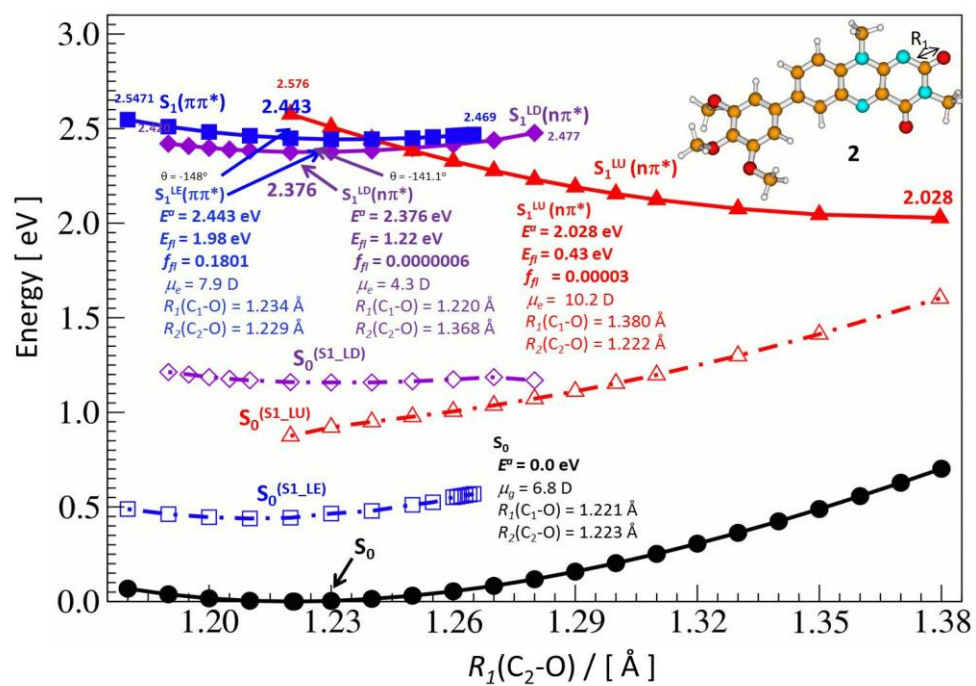
A



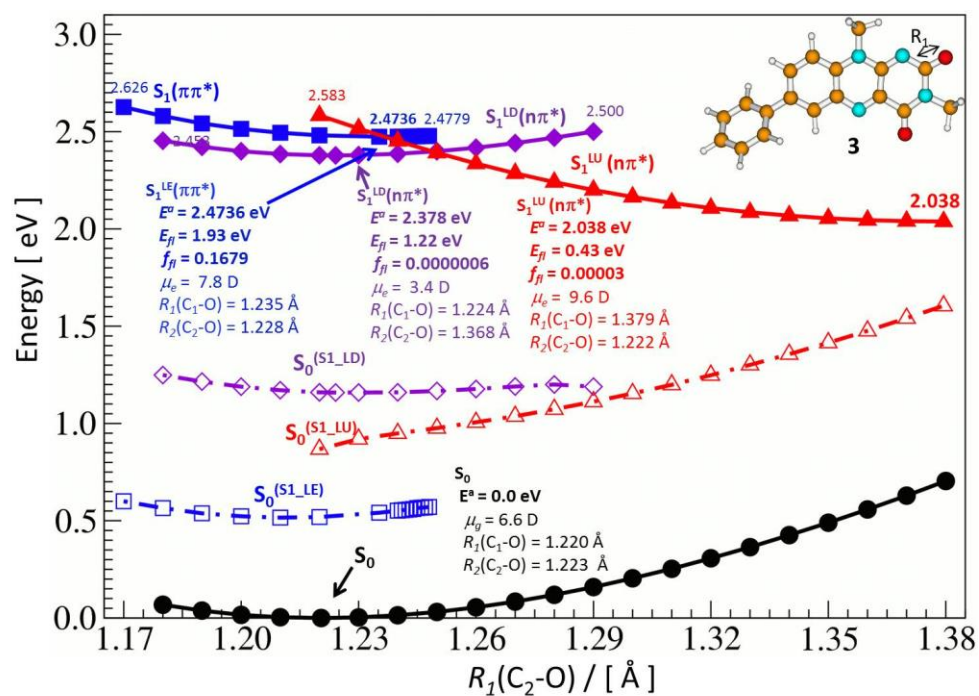
B



c



D



E

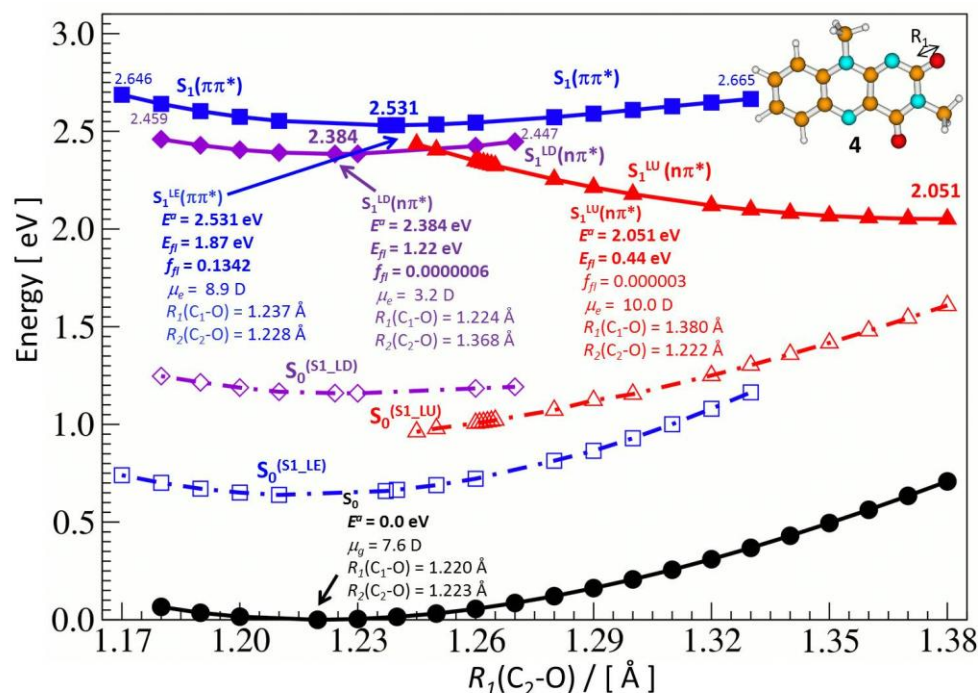
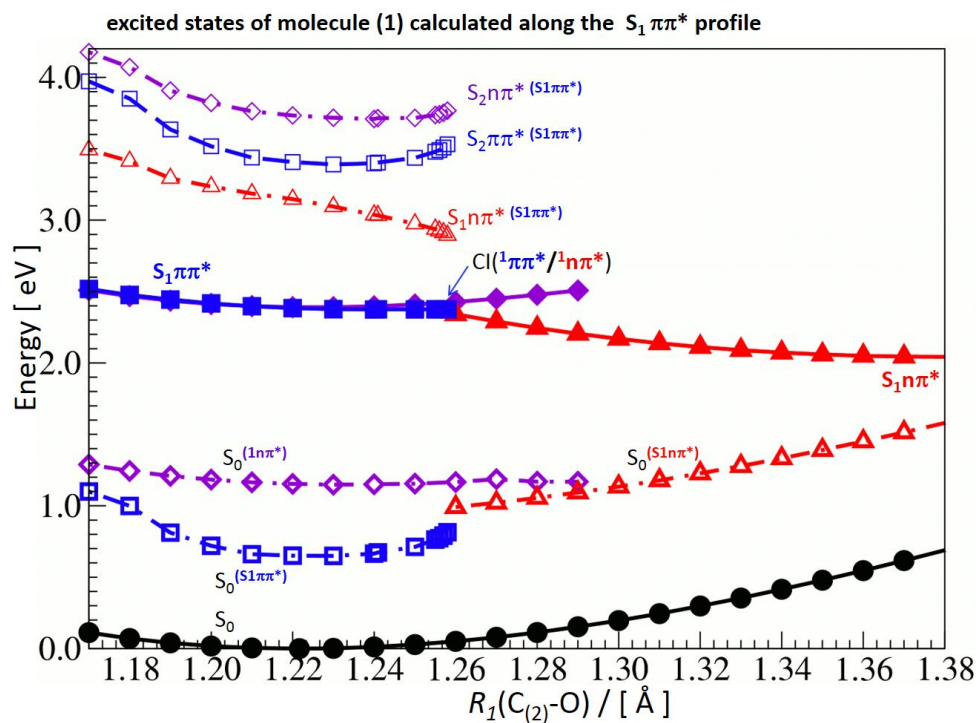
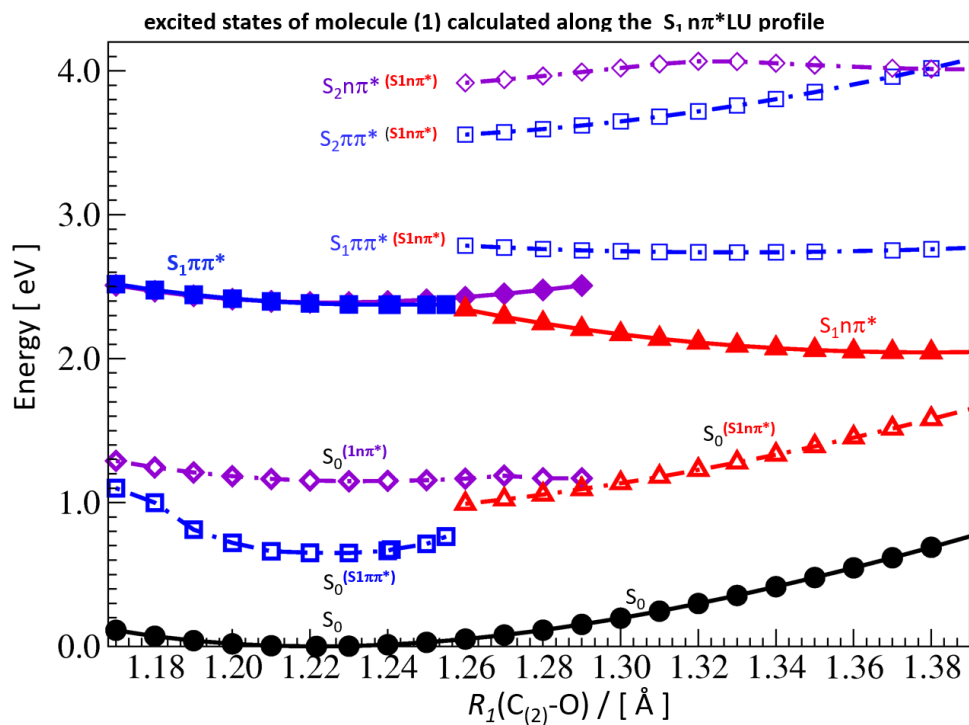


Figure S3. Excited-state (S_1) potential-energy profiles of the compounds **1** in **H-bonded** (A) and **non-H-bonded** isomer (B); **2** (C); **3** (D); and **4** (E) (calculated with the ADC(2)/cc-pVDZ method) plotted as a function of the $R_1(\text{C}_2\text{-O})$ distance coordinate describing the S_1 -state deactivation process through a cascade of the S_1 states leading toward the region with low S_1 - S_0 state energy gap. Solid lines denote the ground (S_0), and excited S_1 -state minimum energy profiles. Dashed lines ($S_0^{S_1}$) denote energy profiles of the ground S_0 state calculated at the optimized geometry of the respective S_1 state. Black circles indicate the S_0 state, blue squares - $S_1(\pi\pi^*)$, violet diamonds - $S_1^{\text{LD}}(n\pi^*)$, and red triangles - $S_1^{\text{LU}}(n\pi^*)$. Equilibrium forms (optimized without any symmetry constraint) of the excited state: $S_1^{\text{LE}}(\pi, \pi^*)$, $S_1^{\text{LD}}(n, \pi^*)$ and $S_1^{\text{LU}}(n, \pi^*)$ are indicated on the profiles by the blue, violet and red arrows, respectively.

A**B**

c

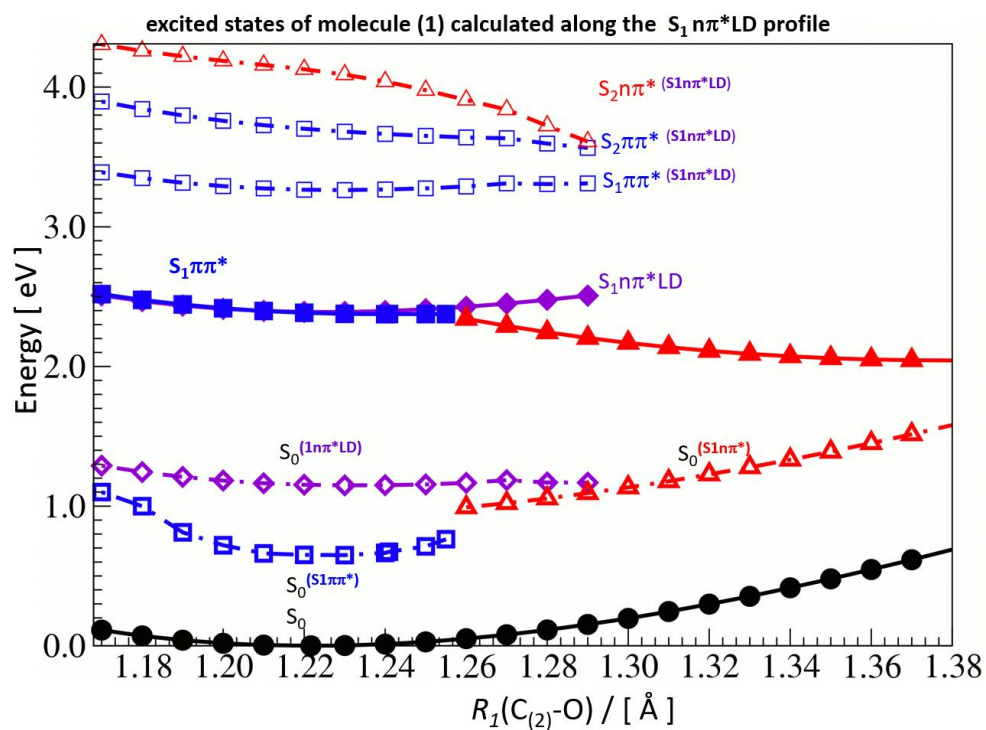


Figure S4. Single-point calculations (ADC(2)/cc-pVDZ) for compound **H-bonded 1** to trace potential-energy profiles of the few lowest excited states in geometry of: $S_1(\pi,\pi^*)$ (Fig. A), $S_1^{\text{LU}}(n,\pi^*)$ (Fig. B), $S_1^{\text{LD}}(n,\pi^*)$ (Fig. C). The $S_1(\pi,\pi^*)$ state profiles are marked with blue open squares, the $S_1^{\text{LU}}(n,\pi^*)$ state profile is marked with red open triangles and the $S_1^{\text{LD}}(n,\pi^*)$ state profile is marked with violet open diamonds. Note in (A) that the conical intersection CI (${}^1\pi,\pi^*/{}^1n,\pi^*$) can be easily reached in a shallow energy curve $S_1(\pi,\pi^*)$.

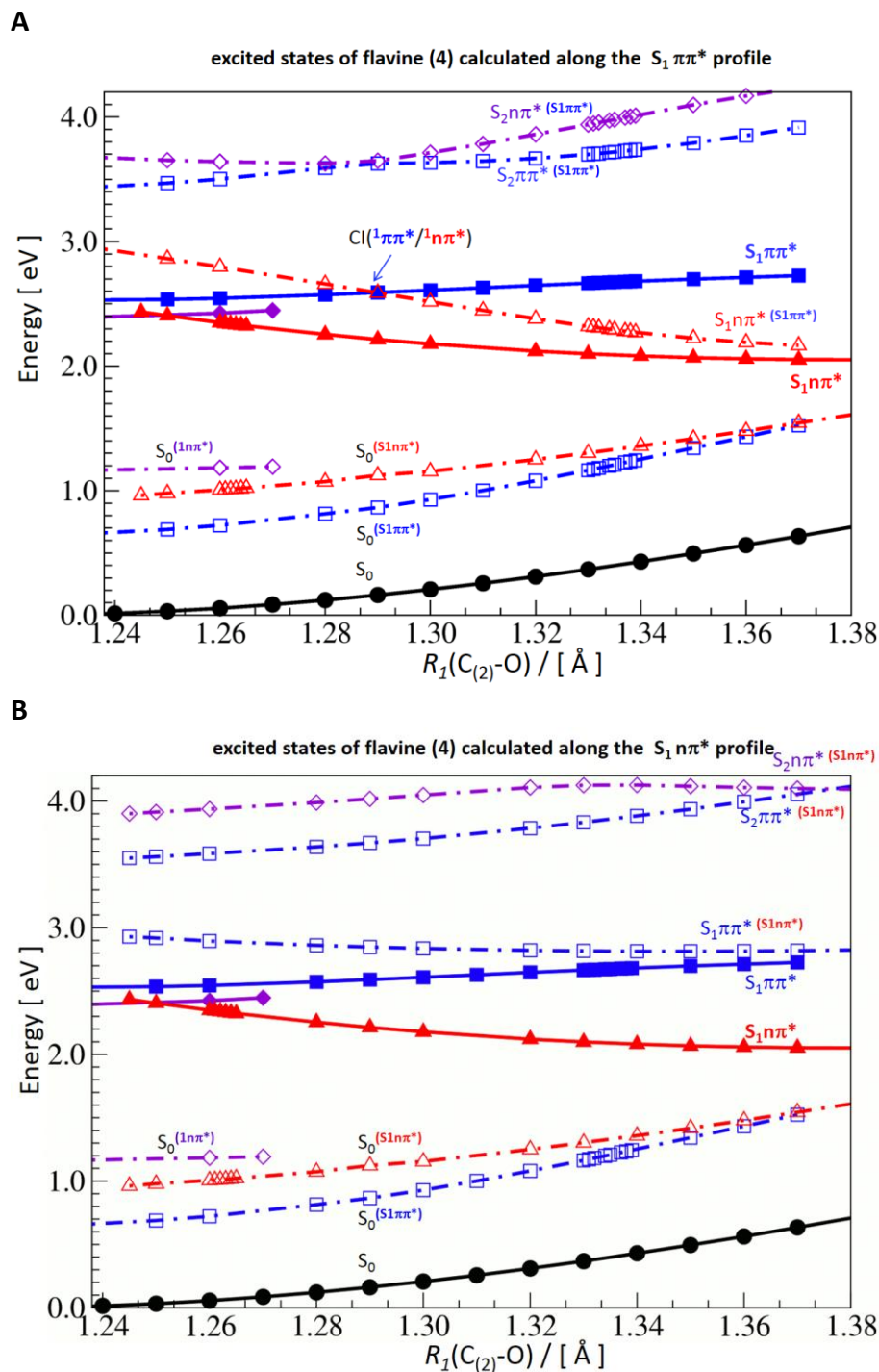
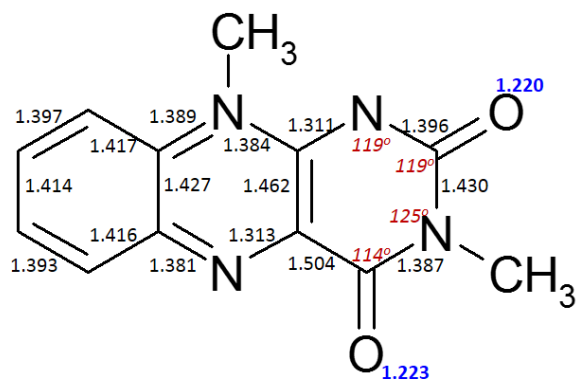


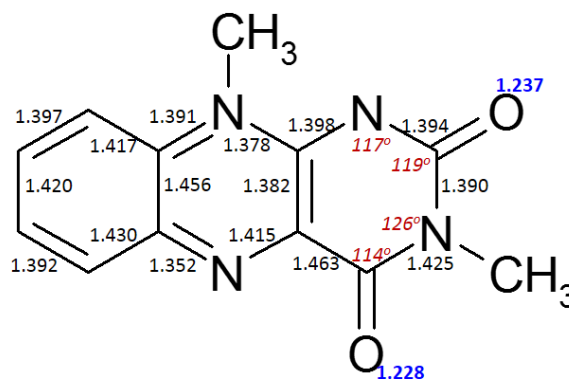
Figure S5. Single-point calculations (ADC(2)/cc-pVDZ) for compound **4** to trace potential-energy profiles of the few lowest excited states in geometry of: $S_1(\pi, \pi^*)$ (A) and $S_1^{LU}(n, \pi^*)$ (B) excited states. The excited-state profiles $S_1(\pi, \pi^*)$ and $S_2(\pi, \pi^*)$ are marked with blue open squares, the state profile $S_1^{LU}(n, \pi^*)$ is marked with red open triangles. Note in (A) that conical intersection $CI(1\pi, \pi^*/1n, \pi^*)$ requires a substantial energy – the $S_1(\pi, \pi^*)$ curve is not shallow, there is an increase in energy upon $C_{(2)}-O$ elongation.

Table S1. Geometrical parameters of the molecule **4** in its equilibrium geometries in its ground electronic and excited states optimized with the MP2/cc-pVDZ method for the state S_0 and with the ADC(2)/cc-pVDZ method for the state S_1 .

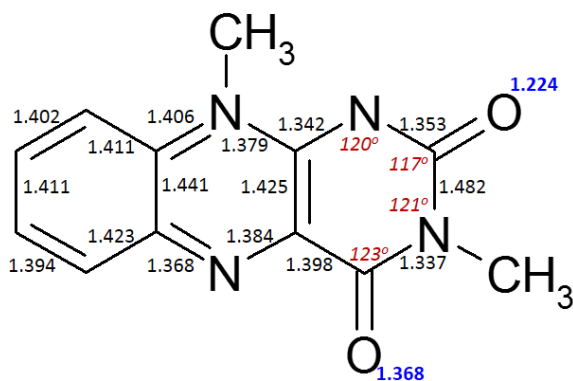
S_0 , MP2/DZ, $\mu_g = 7.56D$



$S_1'(\pi\pi^*)$, ADC(2)/DZ, 2.531 eV $E_{fl} = 1.87$ eV, $\mu_e = 7.13D$



$S_1''(n\pi^*)$ LD, , ADC(2)/DZ, 2.384 eV $E_{fl} = 1.22$ eV, $\mu_e = 3.19D$



$S_1''(n\pi^*)$ LU, ADC(2)/DZ, 2.051 eV $E_{fl} = 0.44$ eV, $\mu_e = 10.0D$

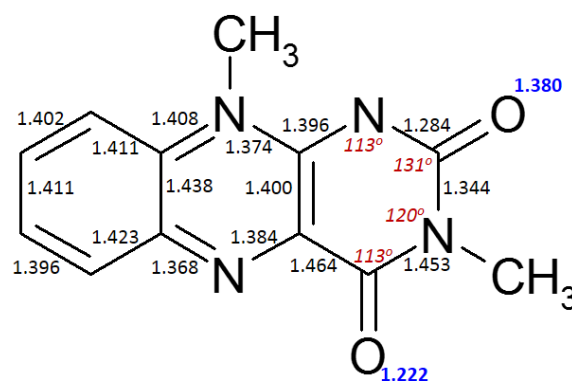


Table S2. Isoalloxazine structure and photophysical properties in acetonitrile accordingly to current study and reported data.

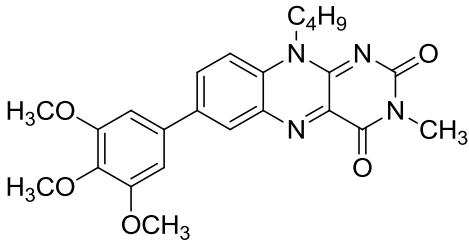
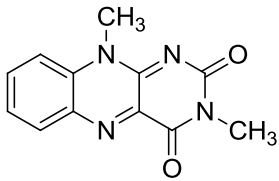
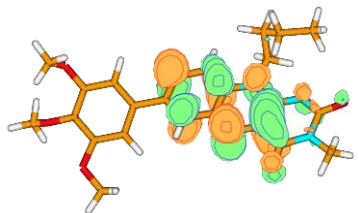
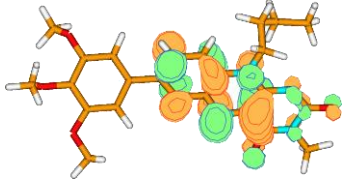
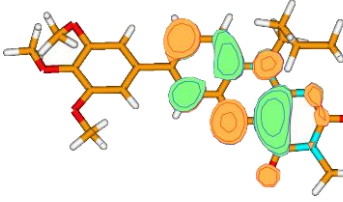
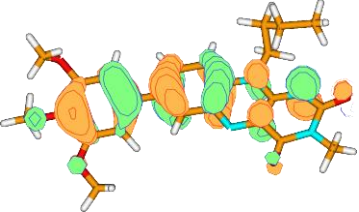
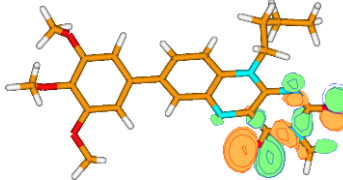
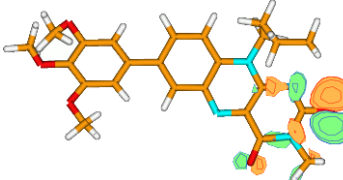
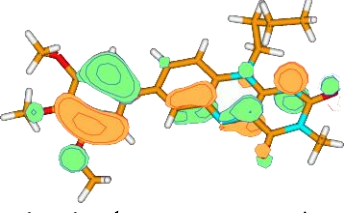
Compound structure	Fluorescence quantum yield Φ_f	$S_1(\pi,\pi^*)$ lifetime τ_{S1}	Reference
 <p>7-(3,4,5-trimethoxyphenyl)isoalloxazine, 1</p>	2.6×10^{-4}	0.5 ps	This study
 <p>3,10-dimethylisoalloxazine, 4</p>	0.35	6.96 ns	Ref. 15

Table S3. Molecular orbitals describing electron excitation for each of the excited-state equilibrium form in the molecule **1**. Adiabatic energy, E^a , and fluorescence energy, E_{fl} , for the given excited-state equilibrium form optimized with the ADC(2)/cc-pVDZ method, given in eV.

$S_1^{LE} (\pi\pi^*)$	$S_1^{LD} (n\pi^*)$	$S_1^{LU} (n\pi^*)$
H-bonded rotamer of 1		
$E^a = 2.374$ eV	$E^a = 2.389$ eV	$E^a = 2.043$ eV
$E_{fl} = 1.70$ eV	$E_{fl} = 1.24$ eV	$E_{fl} = 0.47$ eV
 orbital π^* (LUMO, o120)	 orbital π^* (LUMO, o120)	 orbital π^* (LUMO, o120)
 orbital π (HOMO, o119)	 orbital n (HOMO-5, o114)	 orbital n (HOMO-3, o116)
 orbital π (HOMO-1, o118)		
$-0.76^*[\text{o}(119)\text{->}\text{o}(120)] +$ $+0.40^*[\text{o}(118)\text{->}\text{o}(120)]$	$0.94^*[\text{o}(114)\text{->}\text{o}(120)]$	$0.98^*[\text{o}(116)\text{->}\text{o}(120)]$